

Abiotic and Biotic Compression of Municipal Solid Waste

Christopher A. Bareither¹; Craig H. Benson²; Tuncer B. Edil³; and Morton A. Barlaz⁴

Abstract: This study focused on quantifying relative contributions of abiotic and biotic compression of municipal solid waste (MSW). Abiotic mechanisms include immediate compression, mechanical creep, and moisture-induced waste softening. The biotic mechanism is decomposition of the MSW organic fraction, which when coupled with mechanical creep, yields biocompression. Three 610-mm-diameter laboratory compression experiments were conducted for 1,150 days under the following conditions: (1) waste with no liquid addition (dry), (2) liquid addition spiked with biocide (abiotic), and (3) leachate recirculation (biotic). Immediate compression strain was similar in all three tests (24–27%). Mechanical creep, moisture-induced softening, and biocompression were compared via time-dependent compression ratios (C'_α). Moisture-induced softening occurred in both the abiotic and biotic cells in response to liquid addition and leachate recirculation. Moisture-induced softening accelerated the accumulation of mechanical creep (i.e., approximately doubled C'_α due to mechanical creep relative to the dry cell), but did not increase the overall magnitude. C'_α , in the biotic cell, correlated with the methane flow rate when methanogenesis was controlled by the rate of solids hydrolysis. C'_α , due to mechanical creep in the dry cell and biocompression in the biotic cell, increased exponentially with temperature, and can be represented with an exponential model. C'_α , due to biocompression, was approximately one order of magnitude larger than C'_α due to mechanical creep. DOI: 10.1061/(ASCE)GT.1943-5606.0000660. © 2012 American Society of Civil Engineers.

CE Database subject headings: Municipal wastes; Solid wastes; Settlement; Biological processes; Methane; Recirculation.

Author keywords: Municipal solid waste; Settlement; Bioreactor landfills; Methane generation; Leachate; Recirculation; Biocompression.

Introduction

Settlement of municipal solid waste (MSW) typically consists of three phases: (1) immediate compression, (2) mechanical creep, and (3) biocompression (Bjarngard and Edgers 1990; El-Fadel and Khoury 2000; Park and Lee 1997; Marques et al. 2003; Sharma and De 2007; Sivakumar Babu et al. 2010; Gourc et al. 2010). Immediate compression is an abiotic mechanical process that occurs rapidly in response to an increase in stress. Mechanical creep involves the slow time-dependent abiotic yielding and reorientation of MSW constituents under constant stress, whereas biocompression involves abiotic mechanical creep coupled with biotic decomposition of the MSW organic fraction. Biocompression is primarily associated with anaerobic decomposition of the biodegradable organic fraction of the waste, which depends on the organic content, moisture content, and temperature (Farquhar and Rovers 1973; Barlaz et al. 1990; Chugh et al. 1998; Rao and Singh 2004).

The relative contributions of abiotic and biotic mechanisms are expected to differ depending on how a landfill is operated. In conventional landfills that are operated to minimize moisture infiltration, abiotic mechanical processes are expected to control settlement. In bioreactor landfills, where leachate is recirculated and supplemental liquids are added, both abiotic and biotic processes are expected to contribute to settlement. Predictions of MSW settlement are typically made using models that include parameters representative of these abiotic and biotic processes (Sowers 1973; Bjarngard and Edgers 1990; Edil et al. 1990; El-Fadel and Khoury 2000; Marques et al. 2003; Sivakumar Babu et al. 2010; Gourc et al. 2010).

The primary biodegradable constituents in MSW are cellulose (C) and hemicellulose (H), which comprise approximately 40–60% of MSW by dry weight and account for greater than 90% of its methane potential (Barlaz et al. 1990). MSW decomposition is a microbially mediated process that occurs in sequential phases referred to as hydrolysis, fermentation, acetogenesis, and methanogenesis (Farquhar and Rovers 1973; Zehnder 1978; Barlaz et al. 1989; Pohland and Kim 1999; Levén et al. 2007). The initial step is hydrolysis of complex polymers (e.g., C, H, starch, protein) to lower molecular weight monomers (e.g., sugars, amino acids). Fermentation of these monomers to alcohols, carboxylic acids (e.g., acetate, propionate, butyrate), hydrogen, and carbon dioxide, combined with acetogenesis of hydrogen and carbon dioxide to acetate, yields the substrates and chemical and microbial equilibrium necessary for methanogenesis (Zehnder 1978). In the overall anaerobic decomposition process, hydrolysis is the rate-limiting step when the substrate is complex solid organic material (e.g., C and H), whereas methanogenesis is rate-limiting when the substrate is solubilized (Noike et al. 1985; Pavlostathis and Giraldo-Gomez 1991; Vavilin et al. 1996).

The decomposition phases of MSW have unique leachate chemistry and biogas characteristics that have been linked to time-dependent compression phases of mechanical creep and

¹Research Associate, Geological Engineering, Univ. of Wisconsin-Madison, Madison, WI 53706 (corresponding author). E-mail: bareither@wisc.edu

²Wisconsin Distinguished Professor, Director of Sustainability Research and Education, and Chair, Civil and Environmental Engineering, Geological Engineering, Univ. of Wisconsin-Madison, Madison, WI 53706. E-mail: chbenson@wisc.edu

³Professor, Geological Engineering, Univ. of Wisconsin-Madison, Madison, WI 53706. E-mail: tbedil@wisc.edu

⁴Professor and Head, Dept. of Civil, Construction, and Environmental Engineering, North Carolina State Univ., Raleigh, NC 27695-7908. E-mail: barlaz@ncsu.edu

Note. This manuscript was submitted on February 15, 2011; approved on November 1, 2011; published online on December 10, 2011. Discussion period open until January 1, 2013; separate discussions must be submitted for individual papers. This paper is part of the *Journal of Geotechnical and Geoenvironmental Engineering*, Vol. 138, No. 8, August 1, 2012. ©ASCE, ISSN 1090-0241/2012/8-877–888/\$25.00.

biocompression (Hossain et al. 2003; Olivier and Gourc 2007; Ivanova et al. 2008; Gourc et al. 2010). During initial hydrolysis, fermentation, and acetogenesis (i.e., acid formation phase), carboxylic acids accumulate in the leachate and the leachate hydrogen ion concentration (pH) decreases (Barlaz et al. 1989; Pohland and Kim 1999). Mechanical creep is dominant during the acid formation phase (Wall and Zeiss 1995; Ivanova et al. 2008). Biocompression coincides with methanogenesis, which is characterized by methane generation, acid consumption, and increasing leachate pH. The transition from dominant mechanical creep to dominant biocompression has been linked to the onset of methane generation and acid consumption (Olivier and Gourc 2007; Ivanova et al. 2008; Bareither et al. 2010; Gourc et al. 2010).

Laboratory investigations evaluating the effect of mechanical creep and biocompression on MSW settlement are described in Table 1. These studies included temperature control (Wall and Zeiss 1995), water addition (Kang et al. 1997), and acid addition (Hossain et al. 2003; Ivanova et al. 2008) to isolate the effects of moisture addition and biological activity on MSW settlement. Time-dependent compression rates are represented by a mechanical creep ratio ($C'_{\alpha M}$) and biocompression ratio ($C'_{\alpha B}$), which are defined as the change in strain per change in logarithm of time (Bjargard and Edgers 1990; El-Fadel and Khoury 2000; Hossain and Gabr 2005).

$C'_{\alpha M}$ ranges from 0.015 to 0.07 regardless of experimental conditions (Table 1). The largest $C'_{\alpha M}$ (0.05–0.07) is reported for Kang et al. (1997), and attributed to aggressive liquid addition/leachate recirculation. Wall and Zeiss (1995) also identified a larger contribution of physical compression due to initial liquid addition and presumed softening of waste constituents.

$C'_{\alpha B}$ ranges from 0.10 to 0.35 (Table 1), with the higher end being indicative of enhanced refuse decomposition during methanogenesis. Experiments by Olivier and Gourc (2007) and Ivanova et al. (2008) with leachate recirculation exhibited a transition from mechanical creep to biocompression concurrent with a decrease in volatile fatty acids or chemical oxygen demand (COD), increase in pH, and onset of methane generation.

Of the studies compiled in Table 1, only Olivier and Gourc (2007) and Ivanova et al. (2008) identified immediate compression, mechanical creep, and biocompression on single test specimens with corresponding leachate chemistry and gas generation data. These experiments illustrated abiotic and biotic compression mechanisms, and the chemical and biological characteristics of the MSW. However, controls without leachate addition and recirculation (to simulate conventional cells) and with liquid addition and inhibited biological activity (to separate physical and biochemical compression mechanisms) were not conducted.

In this study, experiments were conducted to quantify abiotic and biotic contributions to MSW settlement, and to relate biotic compression to temperature, leachate chemistry, methane generation, and solids decomposition. Three large-scale laboratory compression tests were conducted under the following conditions: (1) waste with no liquid addition (dry), (2) liquid addition spiked with biocide (abiotic), and (3) leachate recirculation (biotic). The dry and abiotic experiments identified mechanical settlements that can be attributed to physical softening of the waste particles due to moisture addition. The biotic test illustrated the relative magnitudes of mechanical creep in softened MSW and biocompression. The compression tests were operated for 1,150 days. Settlement, gas production and composition, and leachate chemistry were monitored.

Methods and Materials

Municipal Solid Waste

The waste used was collected from a transfer station in Wake County, North Carolina, and contained the following material composition: 56.8% paper, 16.1% plastic, 11.8% food waste, 5.4% soil, 3.5% metal, 3.4% glass, 2.3% textiles, 0.5% miscellaneous, and 0.2% yard waste on a wet mass basis. Each waste fraction was shredded in a high-torque slow-speed shredder to particles sizes ≤ 100 mm. Shredded waste was then recombined proportionately to the initial waste composition.

Composite waste samples recovered at the end of the compression experiments were analyzed for water content; C, H, and

Table 1. Laboratory Experiments Evaluating Effects of Mechanical Creep and Biocompression on Waste Settlement

Reference	Experiment description	Test duration (<i>d</i>)	Cell diameter (mm)	Vertical stress (kPa)	Water content (%)	Temperature (°C)	Weekly liquid dose (L/Mg)	$C'_{\alpha M}$	$C'_{\alpha B}$
Wall and Zeiss (1995)	Leachate recirculation, hydrogen ion concentration buffering, and sewage sludge addition	225	570	10	53.6	25	58	0.033–0.056	—
	Conventional	225	570	10	53.6	4	—	0.037–0.049	—
Kang et al. (1997)	Water addition	320	400	—	96	28	7	0.045	—
	Leachate recirculation	320	400	—	96	28	7, 35, and 161	0.050–0.070	0.10–0.14
Hossain et al. (2003)	Active biodegradation	70	64	95	122	39	—	0.020–0.030	0.05–0.19
	Saturated with 6% acetic acid	20	64	95	122	39	—	0.015–0.030	—
Olivier and Gourc (2007)	Leachate recirculation	660	1,000	130	51	34	6–48	0.046	0.35
Ivanova et al. (2008)	Nutrient/sludge addition and leachate recirculation	919	480	50	—	30	17.2 ^a	0.044	0.13
	10 g/L acetic and propionic acid addition	919	480	50	—	30	17.2 ^a	0.054	0.19

Note: Water content on dry weight basis; $C'_{\alpha M}$ = mechanical creep ratio; $C'_{\alpha B}$ = biocompression ratio.

^aDose in L/Mg/h when in use.

lignin (L) contents; volatile solids (VS); and biochemical methane potential (BMP). Water content was determined by oven drying at 105°C for 24 h or until the change in mass loss was negligible. VS were determined as the mass loss on combustion at 550°C for 2-hour BMP assays were conducted following protocols described in Wang et al. (1994). C, H, and L contents were measured using procedures described in Pettersen and Schwandt (1991) and Davis (1998). Sugars resulting from hydrolysis of C and H were analyzed by high-performance liquid chromatography using an electrochemical detector. All chemical tests were conducted on material ground to pass a 1-mm screen.

Laboratory Reactors

Compression tests were conducted in 610-mm-diameter by 900-mm-tall stainless steel cells. A schematic of a compression cell is shown in Fig. 1. Gravel was placed at the base of the cell for leachate collection, and on top of the waste for stress application (8 kPa) and liquid distribution. A fine-mesh polyethylene screen was placed between the waste and drainage gravel to prevent clogging of the effluent port. A nonwoven needle-punched geotextile was placed on top of the waste specimen to equalize liquid distribution in the abiotic and biotic tests. Liquid distribution systems consisting of perforated acrylic pipes were placed on top of the gravel layer in the abiotic and biotic cells (Fig. 1). The cell lid was secured to the tank with bolts and sealed with a silicon sealant.

Waste settlement was measured via aluminum settlement rods connected to perforated stainless-steel plates placed on top of the waste (Fig. 1). Settlement was monitored during placement of the gravel surcharge with tapes affixed to the settlement rods, and with dial gages fixed to the test cell lids after sealing the cells. A greased rubber stopper was placed between the settlement rod and cell lid to create a gas-tight seal and allow free displacement of the settlement plate. Settlement strain was computed with respect to the waste thickness after preparation of each specimen. Time-dependent compression ratios (C'_a) were obtained from least-squares linear regression of strain versus logarithm of the time data.

Ambient air temperature in the laboratory was monitored throughout the duration of the experiment. Air temperature is used as an indicator of waste temperature in the three laboratory reactors.

A summary of the initial waste thickness, dry unit weight, and dry weight water content for the three test cells is given in Table 2.

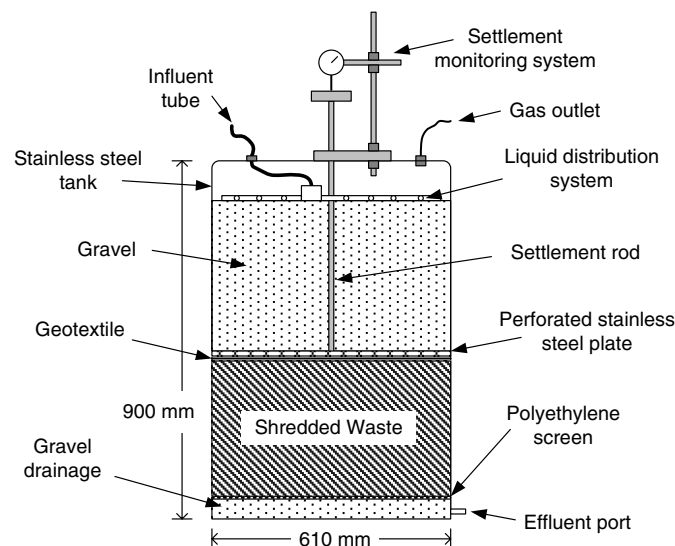


Fig. 1. Schematic of laboratory compression cell

Table 2. Initial Waste Thickness, Initial and Final Waste Dry Unit Weight and Dry Weight Water Content, Total Liquid Added, and Estimated Solids Loss Because of Decomposition for the Dry, Abiotic, and Biotic Specimens

Characteristic	Dry	Abiotic	Biotic
Initial waste thickness (mm)	345	335	335
Initial dry unit weight (kN/m ³)	2.03	2.10	2.02
Initial dry weight water content (percentage)	57	55	62
Total liquid added (L)	0	462.0	466.7
Final dry weight water content (percentage)	61	158	174
Estimated solids loss from decomposition (kg)	0.007 ^a	0	6.96 ^b
Final dry unit weight (kN/m ³) ^c	3.09	3.10	2.89

^aBased on methane production in dry reactor.

^bBased on cellulose and hemicellulose loss as described in the text.

^cAccounts for solids loss due to decomposition.

Prior to loading each cell, the shredded and reconstituted waste was thoroughly mixed and split in thirds to obtain specimens with similar waste composition. A total waste mass of 32.6 kg was used for each specimen and compacted via hand tamping in three equal layers. The initial waste thickness was approximately 340 mm, dry unit weights (γ_d) ranged between 2.02 and 2.10 kN/m³ (~ 0.21 Mg/m³), and dry weight water content (w_d) ranged between 55 and 62% (Table 2).

Liquid Management

Liquid addition in the abiotic and biotic tests began on Day 22 at a rate of 2 L per day. Liquid addition/recirculation was maintained at 2 L per day between 22 and 120 days to achieve field capacity of the waste specimens (i.e., volume out/volume in ≈ 1). After reaching field capacity, the liquid addition/recirculation rate was decreased to 2 L per week for the duration of the experiment.

Deionized (DI) water was initially added to the biotic cell (no microbial seeding). After leachate generation began, leachate was recirculated with additional DI water added, if necessary, to achieve the target recirculation volume. Recirculated leachate was buffered with a 6 M NaOH solution until the effluent pH was > 7 to prevent acidic conditions that can inhibit methanogenesis. Leachate collected during days without recirculation was stored in a zero-headspace container at 4°C to minimize biological activity.

Liquid added to the abiotic cell consisted of DI water spiked with Dovicil QK-20, a commercially available antimicrobial agent from The Dow Chemical Company (Midland, MI). Dovicil QK-20 contains 2,2-dibromo-3-nitropropionamide (DBNPA) as the active antimicrobial chemical. Fresh mixtures of DI water with 2,000 mg/L DBNPA were added for each liquid addition in the abiotic cell.

Leachate samples were collected every 1–2 days for the first 100 days of liquid addition and leachate recirculation, and decreased thereafter to every 1–2 weeks. Chemical parameters measured on leachate samples included pH, electrical conductivity (EC), oxidation-reduction potential (ORP), COD, and alkalinity. pH, EC, and ORP were measured on a Fisher Scientific (Waltham, MA) AR60 m with Microelectrodes, Inc. (Bedford, NH) probes for pH (MI-410) and ORP (MI-800/410), and a Fisher Scientific Accumet conductivity cell for EC (13–620–155). COD was measured using a HACH (Loveland, CO) 0–1,500 mg/L COD test kit. Standard COD curves were created with potassium hydrogen phthalate solution and all absorbance measurements were completed with a Spectronic 20 Genesys spectrophotometer (Sigma-Aldrich Co., St. Louis, MO) at a 600-nm wavelength. Alkalinity was determined by titration with a 0.1-N H₂SO₄ solution in accordance with Standard Methods (1999).

Gas Collection and Composition

Gas composition was assessed weekly at the start of the experiment by sampling gas from the headspace of the reactors (Fig. 1) and analyzing its composition with a Shimadzu Gas Chromatograph (GC-2014) equipped with flame ionization and thermal conductivity detectors. Percentages of hydrogen, nitrogen, oxygen, carbon dioxide, and methane were calculated with respect to standard gases (Scott Specialty Gases, Plumsteadville, PA; AGA Gas, Inc., Maumee, OH).

Problems encountered with the gas collection systems during the first 255 days rendered data from this period erroneous and unusable. The gas collection systems were then improved and reliable data were subsequently obtained. Gas was captured in 40-L flexfoil SKC Inc. (Eight Four, PA) gasbags, and volume was measured via water displacement in calibrated 50-L (± 0.5 L) or 10-L (± 0.1 L) containers submerged in acidified water (pH ~ 3.0). Gas samples for composition analysis were extracted from the gasbags and stored in evacuated glass vials prior to analysis.

Results

Settlement

Cumulative settlement strain versus time for the dry, abiotic, and biotic cells is shown in Fig. 2. A summary of cumulative waste settlement and percent strain corresponding to immediate compression, mechanical creep, and biocompression for the three test cells is presented in Table 3. Total waste settlement in the biotic cell (179.8 mm = 54% of initial thickness) was 56% greater than settlement in the dry cell and 69% greater than settlement in the abiotic cell. The significant increase in settlement in the biotic cell that occurred between 200 and 1,150 days (Fig. 2) is attributed to biocompression (described subsequently).

Gravel, used for stress application and liquid distribution, was placed on top of each specimen during the first day to achieve an 8 kPa creep stress (shown as duration of stress application in Fig. 2). Immediate compression during this stress increase was similar for the dry and biotic cells (Fig. 2). Less strain

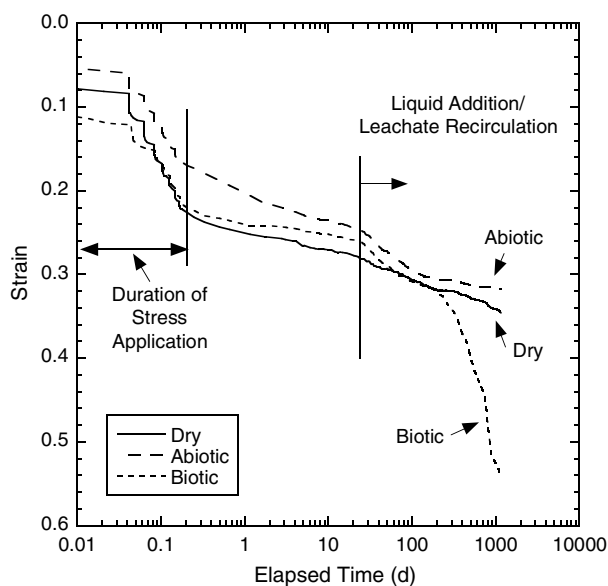


Fig. 2. Cumulative strain versus time for the dry, abiotic, and biotic compression tests

Table 3. Compression Summary for Dry, Abiotic, and Biotic Tests

Metric	Dry	Abiotic	Biotic
Cumulative settlement (mm)	118.800	106.500	179.800
Cumulative strain	0.340	0.320	0.540
Immediate compression strain (strain at 10 days)	0.270	0.240	0.250
Cumulative time-dependent compression strain (10–1,150 days)	0.075	0.083	0.290
Mechanical creep and softening strain (10–150 days)	0.044	0.068	0.063
Mechanical creep and biocompression strain (150–1,150 days)	0.031	0.015	0.230

Note: All strains computed with respect to initial waste thickness.

accumulated immediately following stress application in the abiotic cell, perhaps due to the modestly higher initial dry unit weight of this specimen (Table 2). Accumulation of strain in the abiotic cell continued at a higher rate until approximately 5–10 days (Fig. 2). After 10 days, the compression behavior in all three cells was similar, and strain accumulated as of 10 days was attributed to immediate compression. Strain due to immediate compression was comparable in all three cells: 0.27 for the dry cell, 0.24 for the abiotic cell, and 0.25 for the biotic cell (Table 3).

Time-dependent compression strain and C'_α for the dry, abiotic, and biotic cells are shown in Fig. 3(a). Cumulative time-dependent compression strain between 10 and 1,150 days in the dry and abiotic cells was similar (Fig. 3), and approximately 0.08 (Table 3). Cumulative time-dependent strain in the biotic cell was 0.29 (Table 3), which is more than 3.5 times the strain accumulated during the same period in the dry and abiotic cells.

Abiotic Waste Settlement

Time-dependent compression strain and C'_α for the dry, abiotic, and biotic cells between 10 and 200 days are shown in Fig. 3(b). Prior to liquid addition in the abiotic and biotic cells (Day 22), C'_α was similar for all three cells and ranged between 0.027 and 0.037. These values for C'_α are comparable with the range of $C'_{\alpha M}$ in Table 1, and indicate that similar mechanical creep compression was occurring in all three cells. With the onset of liquid addition to the abiotic and biotic cells, C'_α increased relative to the dry cell [Fig. 3(b)] due to moisture-induced softening. Moisture softens porous waste constituents (e.g., paper, cardboard), decreasing stiffness of the waste matrix and increasing compression. A similar effect was observed for laboratory-scale experiments by Wall and Zeiss (1995) and Kang et al. (1997) and in a field-scale experiment by Bareither et al. (2012). Following 4 months of liquid addition and leachate recirculation (elapsed time = 121 days), C'_α for the three cells were again comparable, ranging from 0.038 to 0.043.

Moisture-induced softening increased the compression strain in the abiotic and biotic cells ($\sim 2\%$ additional strain) between 10–150 days, relative to the dry cell (Table 3). This softening effect was finite, because the increased rate of compression lasted only 3 months [Fig. 3(b)]. The additional rate of compression are likely functions of waste composition and liquid dose rate. Waste with greater proportions of paper, cardboard, textiles, and other materials with stiffness sensitive to wetting will yield larger compression strains as a result of moisture-induced softening. A positive correlation

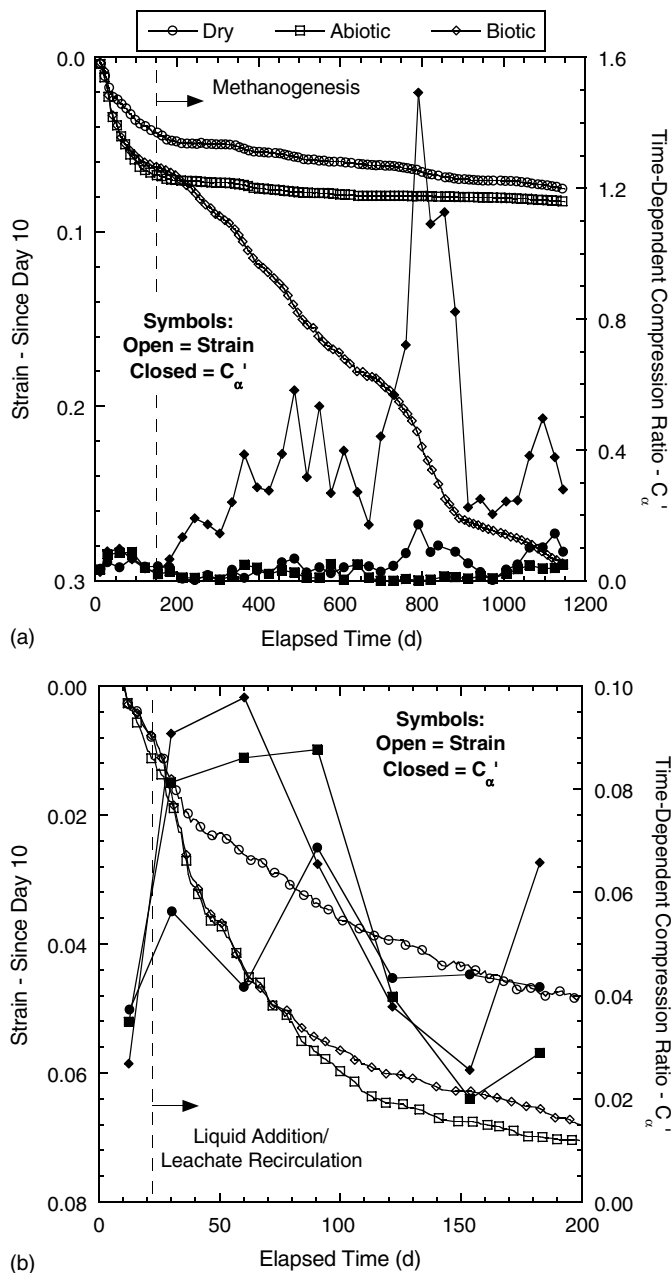


Fig. 3. Cumulative strain since Day 10 and monthly time-dependent compression ratios for the dry, abiotic, and biotic test cells between (a) 10 and 1,150 days; (b) 10 and 200 days; Note: 10% of daily strain data are shown in a and 20% are shown in b

between C'_α and the leachate dose rate was reported by Bareither et al. (2010) for full-scale bioreactor landfills.

Following the increase in strain attributed to moisture-induced softening, C'_α in the abiotic cell decreased and minor amounts of strain accumulated between 150 days and the end of the experiment [Fig. 3(a)]. However, time-dependent compression in the dry cell occurred at approximately a consistent linear rate with respect to the logarithm of time (Fig. 2). Even though moisture-induced softening in the abiotic cell initially increased the rate and magnitude of time-dependent compression, total time-dependent strains accumulated in the dry (0.075) and abiotic (0.083) cells were comparable [Fig. 3(a) and Table 3]. Thus, moisture-induced softening accelerates the accumulation of abiotic mechanical creep, but does not increase the total magnitude.

Biotic Waste Settlement

Waste settlement attributed to biotic mechanisms occurred in both dry and biotic cells, although settlement in the biotic cell was much larger. The transition from mechanical creep to biocompression in the biotic cell occurred between 180 and 200 days, identified in Figs. 3(a) and 3(b) by the change in slope of the strain versus time relationship and corresponding increase in C'_α . A similar transition was not identified in the dry cell due to relatively minor waste decomposition (described subsequently).

The magnitude and rate of compression increased significantly in the biotic cell in response to biocompression. At the end of the experiment (i.e., 1,150 days), strain attributed to biocompression was 0.23 (Table 3) and accounted for 42% of the total strain measured in the biotic cell. During this same period, strain accumulated in the dry cell (0.031) accounted for less than 10% of the total strain.

Leachate Chemistry

Temporal trends of leachate pH, COD, ORP, EC, and alkalinity for the abiotic and biotic cells are shown in Fig. 4. Liquid addition began on Day 22 at 2 L per day, and the first effluent samples from both cells were collected on Day 29. To the authors' knowledge, no studies have used the biocide employed in this study to inhibit biological activity in MSW. Thus, the trends in abiotic leachate chemistry are limited to comparisons with the biotic cell, and are not compared with other leachate data for MSW.

Biotic Cell

The leachate pH from the biotic cell climbed steadily throughout the experiment from 5.1 initially to approximately 9 at the end of the experiment. The early rise in pH [Fig. 4(a)] was facilitated by the neutralization of recirculated leachate between 29 and 175 days (to prevent acid-stuck conditions). Increases in pH after 175 days were due to acid consumption and subsequent generation of methane and carbon dioxide (described subsequently).

Alkalinity, EC, and COD increased with initial leachate recirculation and then began to decrease at approximately 150 days [Figs. 4(b), 4(d), and 4(e)]. Similar temporal behavior has been reported by Ham and Bookter (1982) for EC and COD and by Pohland (1980) and Bilgili et al. (2007) for alkalinity. ORP of leachate from the biotic cell initially increased and then began decreasing at approximately 1.5 mV/d. ORP became negative at 150 days and diminished to approximately -200 mV. After approximately 400 days, the ORP began to increase, and then stabilized at 21 ± 55 mV between 500 days and the end of the experiment [Fig. 4(c)]. Negative ORP between 150 and 500 days corresponded with high COD removal rate (101 mg/L/d), whereas positive ORP between 500 and 1,150 days corresponded with low COD removal rate (6 mg/L/d) [Figs. 4(b) and 4(c)].

The initial high COD concentrations ($> 25,000$ mg/L), acidic pH, and positive ORP between 29 and 150 days correspond to the initial phase of solids hydrolysis and fermentation. Relatively minor amounts of C and H hydrolysis occur during this phase of acid formation (Barlaz et al. 1989), and compression in the biotic cell was attributed to mechanical creep and moisture-induced softening. The increasing pH near 7 [Fig. 4(a)], transition to decreasing COD concentration [Fig. 4(b)], and transition to negative ORP [Fig. 4(c)] at approximately 150 days (marked by dashed lines) corresponds to the onset of methanogenesis (Barlaz et al. 1989; Kim and Pohland 2003; Olivier and Gourc 2007). C'_α in the biotic cell began increasing following this transition in leachate chemistry, which suggests a transition from mechanical creep to biocompression [Fig. 3(a)].

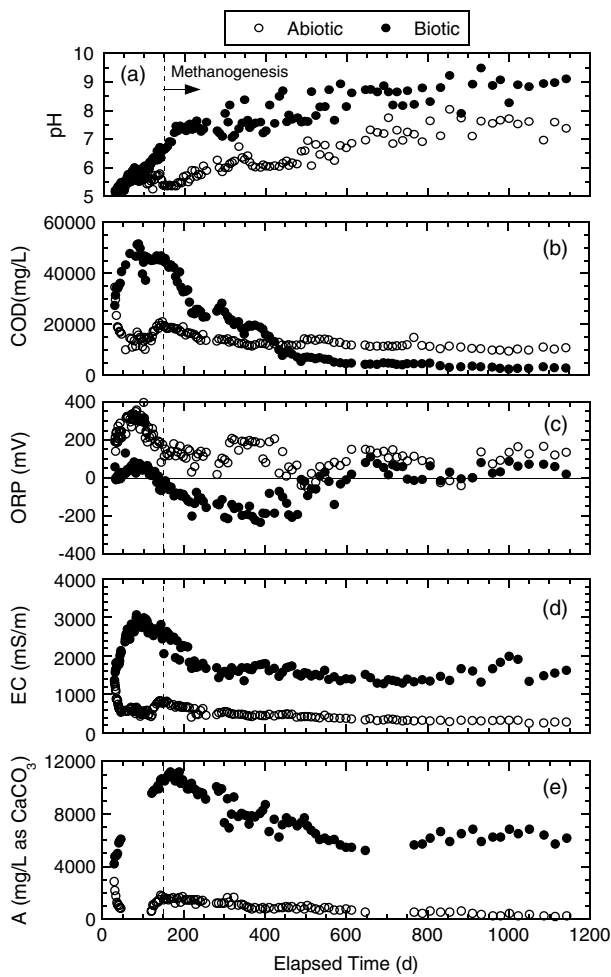


Fig. 4. Temporal trends of (a) leachate hydrogen ion concentration (pH), (b) chemical oxygen demand (COD), (c) oxidation-reduction potential (ORP), (d) electrical conductivity (EC), and (e) alkalinity (A) for the abiotic and biotic test cells; dashed lines indicate transition to methanogenesis; Influent biocide had hydrogen ion concentration 4.4, chemical oxygen demand = 10,100 mg/L, oxidation-reduction potential = 400 mV, and electrical conductivity = 40 mS/m; alkalinity was indeterminate by acid titration because influent hydrogen ion concentration was < 4.5

The transition at 500 days marks a change in microbiological and waste decomposition processes. Prior to 500 days, high COD removal corresponds to the accelerated methane production phase, when methanogenic and acetogenic microbial populations proliferate due to the abundance of readily available substrates in the leachate. The transition at 500 days to low COD removal coincides with a shift to decelerated methane production (see the subsequent discussion of methane data). During the decelerated methane production phase, accumulation of carboxylic acids (i.e., increasing COD) does not occur due to a balance between hydrolytic, fermentative, acetogenic, and methanogenic microbial populations. The rates of C and H decomposition increase during this phase and the rate of solids hydrolysis controls the rate of methane generation (Barlaz et al. 1989).

Abiotic Cell

Leachate chemistry for the abiotic cell did not display trends evident of waste decomposition. The pH increased throughout the experiment, even though fresh biocide (pH 4.4) was added with

each dose [Fig. 4(a)]. This pH increase is attributed to the buffering capacity of the MSW and limestone gravel used for liquid distribution and collection. COD concentrations decreased initially, rose modestly between 100 and 150 days, and then decreased gradually for the remainder of the experiments at a rate of approximately 7 mg/L/d [Fig. 4(b)]. The absence of waste decomposition (supported subsequently) suggests that the COD measured in the abiotic cell can be attributed to the leaching of soluble compounds from the waste. EC and alkalinity exhibited similar trends to COD [Figs. 4(d) and 4(e)]. ORP increased initially and then diminished until approximately 300 days. Thereafter, ORP remained approximately constant between -50 and 200 mV. The ORP was generally positive throughout the experiment [Fig. 4(c)].

Methane Generation

Approximately 13% methane was initially detected in the headspace of the biotic cell after 113 days. Methane increased to 55% after 300 days, and then fluctuated between 55 and 65% for the duration of the experiment, with the balance being carbon dioxide. Approximately 5% methane was first detected in the dry cell after 359 days. Throughout the duration of the experiment, methane was never > 8% of the gas composition in the dry cell, and cumulative methane yield in the dry cell was 0.14 L-CH₄/kg-dry. Biogas was never generated in the abiotic cell and methane was never detected in the headspace, which documents the effectiveness of the added antimicrobial agent.

Monthly average methane flow rates and cumulative methane yield for the biotic cell are shown in Fig. 5. The total methane yield from the biotic cell between 255 and 1,150 days was 68.7 L-CH₄/kg-dry. The drop in the methane flow rate between 365 and 500 days (Fig. 5) coincides with high COD removal and the tail-end of the accelerated methane production phase (Barlaz et al. 1989; Kim and Pohland 2003). The relatively low methane flow rate between 500 and 650 days corresponds to low COD removal and a transition to decelerated methane

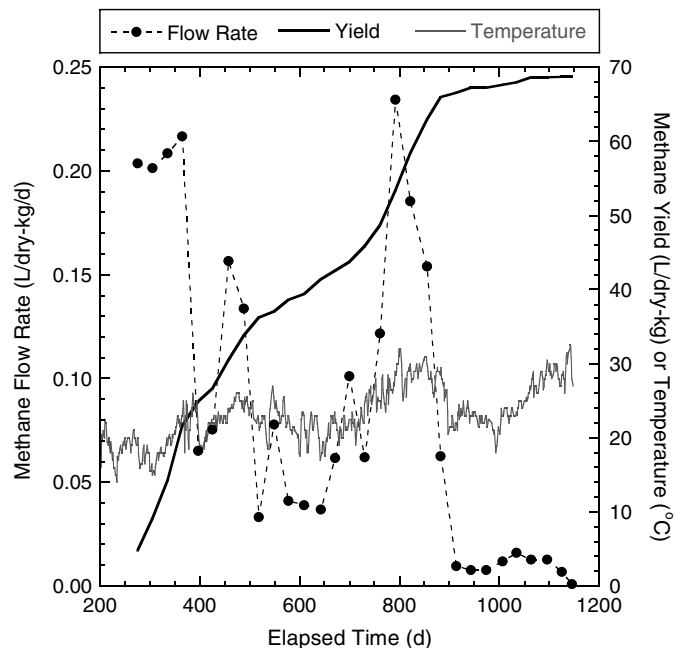


Fig. 5. Relationships of monthly average methane flow rates, cumulative methane yield, and laboratory temperature versus time for the biotic test cell; Note: initial methane detection on Day 113; gas collection data from 255 to 1,150 days

production. A second spike in methane flow rate was recorded on Day 791, which coincided with an increase in laboratory temperature (Fig. 5). This spike in methane generation diminished when the room temperature decreased. Similar correspondence between methane generation and temperature has been reported by others (Hartz et al. 1982; Cecchi et al. 1992; Hao et al. 2008). Room temperature increased again after Day 1,000; however, the methane flow rate continued to diminish, indicating depletion of degradable solids.

The influence of temperature on methane flow rate during high (< 500 days) and low COD (> 500 days) removal phases is shown in Fig. 6. Methane flow rates in Fig. 6 are discrete measurements recorded during testing that were used to compile the monthly averages shown in Fig. 5. During high COD removal, when substrates for methanogenesis were readily abundant in the leachate, the methane flow rate was unrelated to temperature. In contrast, when the availability of soluble substrates was low (i.e., low COD between 500 and 1,150 days), methane flow rate increased with increasing temperature (Fig. 6).

The methane flow rate and temperature relationships in Fig. 6 suggest that temperature has a more pronounced impact on methane generation from MSW when methanogenesis is dependent on the rate of hydrolysis, and directly related to the rate of solids decomposition. Microbial populations and corresponding bioprocesses involved in C hydrolysis (Westlake et al. 1995), fermentation and acetogenesis (Cecchi et al. 1992), and methanogenesis (Kettunen and Rintala 1997) have all been shown to be temperature sensitive with optimal mesophilic temperatures near the upper-end of the mesophilic range (~37–42°C). During high COD removal (i.e., accelerated methane production) relatively little solid hydrolysis occurs and methane production is due to consumption of substrate present in the liquid phase. However, with the transition to decelerated methane production and low COD removal, the rate of methane generation depends on the rate of solids hydrolysis (Barlaz et al. 1989). Because hydrolysis is the initial step in anaerobic

decomposition of organic material and is rate-limiting when the major substrate is C and H (Noike et al. 1985; Pavlostathis and Giraldo-Gomez 1991; Vavilin et al. 1996), the positive correspondence between methane flow rate and temperature during low COD removal suggests that hydrolysis is more temperature sensitive than methanogenesis.

The relationship between C'_α and methane flow rate is shown in Fig. 7. The trend lines relating C'_α and methane flow rate were obtained by a linear least-squares regression. The slope of the regression is not significant at the 5% level for the high COD removal phase ($p = 0.32$), which indicates negligible correspondence between C'_α and methane flow rate. In contrast, the slope of the regression for the low COD removal phase is statistically significant ($p = 10^{-6}$), indicating that C'_α increases with methane production during low COD removal.

The increase in methane production during high COD removal only impacts the liquid phase and does not directly translate to enhanced solids decomposition. However, an increase in methane production during low COD removal directly corresponds to an increase in solids hydrolysis, and translates to enhanced solids decomposition, accelerated waste compression, and larger C'_α . This observation, combined with those from Fig. 6, suggest that maintaining elevated temperatures (near optimal) throughout the waste decomposition process in bioreactor landfills is important to realizing the full potential of enhanced methane generation and waste settlement.

For both regressions in Fig. 7, the intercepts are statistically significant and similar (0.36 for high COD removal and 0.35 for low COD removal). This similarity between the intercepts, which corresponds to the absence of methane generation (and biotic waste decomposition), indicates that physical compression mechanisms occurring during periods of high and low COD removal are comparable.

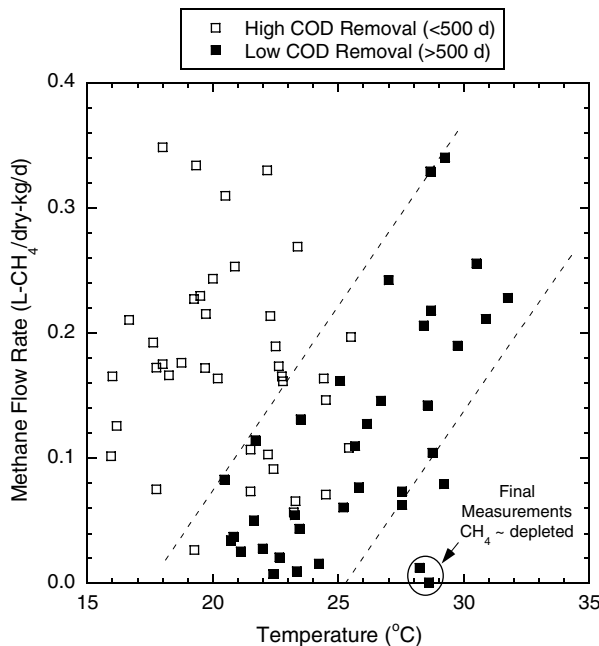


Fig. 6. Methane flow rate versus temperature in the biotic test cell for discrete methane flow rate measurements; data sets correspond to periods of high chemical oxygen demand removal from the leachate (< 500 days) and low chemical oxygen demand removal (> 500 days)

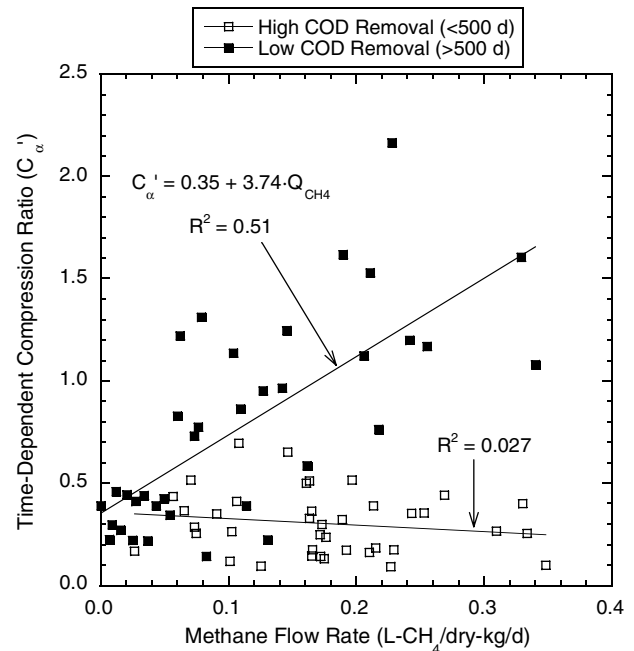


Fig. 7. Relationship between time-dependent compression ratio (C'_α) and methane flow rate (Q_{CH_4}) in the biotic test cell for individual methane flow rate measurements; data sets correspond to periods of high chemical oxygen demand removal from the leachate (< 500 days) and low COD removal (> 500 days)

Waste Composition and Characteristics

A summary of the final γ_d and w_d , total liquid added, and solids loss due to waste decomposition for the dry, abiotic, and biotic test cells is in Table 2. Total liquid addition to the abiotic and biotic cells was similar; 462.0 L was added to the abiotic cell and 466.7 L was added to the biotic cell. This liquid addition amounted to approximately 14,240 L/Mg of MSW, which is approximately 14 times greater than the upper-end of liquid addition realized in full-scale bioreactor landfills (Bareither et al. 2010). The final w_d for the abiotic and biotic cells increased by more than 100% (Table 2) due to liquid addition and leachate recirculation. In contrast, the initial and final w_d for waste in the dry cell differed by only 4%, which is within the variability commonly associated with MSW water content measurements (Hull et al. 2005; Bareither et al. 2010).

Photographs of the dry, abiotic, and biotic wastes exhumed at the end of reactor operation are shown in Fig. 8. Materials in the dry and abiotic wastes were visually identifiable, with print on paper constituents still legible. Waste exhumed from the biotic cell was



Fig. 8. (Color) Municipal solid waste recovered from (a) dry; (b) abiotic; and (c) biotic test cells at the end of reactor operation

darker in appearance and individual material constituents were difficult to identify. Chemical characteristics of the waste samples are summarized in Table 4. The final VS, C and H contents, $[C + H]/L$, and BMP in the biotic cell are all lower than those in the dry and abiotic cells due to waste decomposition. Waste in the biotic cell became enriched in L, which is recalcitrant in anaerobic environments (Colberg 1988). Minimal methane was generated from the dry cell (0.14 mL-CH₄/g-dry), which corresponds to minimal solids decomposition. The similarity between the VS, C and H contents, and $[C + H]/L$ between the dry and abiotic cells, along with the absence of methane in the abiotic cell, confirms that the biocide effectively inhibited biological activity in the abiotic cell.

Initial solid waste samples were not analyzed; however, initial chemical characteristics can be assumed similar to those of the final BMP for the dry cell and final C, H, and L content for the dry and abiotic cells (Table 4). These C, H, and L content correspond to $[C + H]/L$ ratios of 2.55 and 2.88, which are typical of fresh MSW (Barlaz 1997). The low BMP for the final abiotic waste (Table 4) is due to saturation with biocide, which inhibited biological activity during the BMP assay.

The mass loss due to decomposition in the biotic cell (Table 2) was computed as the difference between the average C and H content from the dry and abiotic cells and those of the biotic cell, multiplied by the initial dry waste mass of the biotic cell. Accounting for this solids loss due to decomposition, the final γ_d in the biotic cell was 2.89 kN/m³, whereas the final γ_d in the dry and abiotic cells was approximately 3.10 kN/m³ (Table 2). The theoretical methane yield corresponding to C and H removal in the biotic cell, assuming complete conversion of the measured C and H loss to methane and carbon dioxide (Barlaz 2006), is 139 mL-CH₄/g-dry. This theoretical methane yield is similar to the difference between the dry and biotic final BMP assays (147 mL-CH₄/g-dry), and suggests that methane generation in the biotic cell occurred predominantly from C and H decomposition. The difference between the BMP for the dry and biotic cells also indicates that 92% of the methane embodied in the MSW was removed in the biotic cell.

Relative Contributions of Abiotic and Biotic Compression

Relationships between C'_α and temperature for the dry, abiotic, and biotic cells are shown in Fig. 9. Exponential regression lines in Fig. 9 are of the form

$$C'_\alpha = \beta \times e^{(\lambda \times T)} \quad (1)$$

where T = temperature (°C) and β and λ = regression parameters. A summary of the regression parameters and statistical significance is presented in Table 5.

Table 4. Cellulose, Hemicellulose, and Lignin Contents, $[C + H]/L$ Volatile Solids, and Biochemical Methane Potential for Final Waste Samples from the Dry, Abiotic, and Biotic Test Cells

Characteristic	Dry	Abiotic	Biotic
Cellulose (percentage)	42.70	43.80	14.00
Hemicellulose (percentage)	9.40	10.10	5.50
Lignin (percentage)	20.40	18.70	39.30
$[C + H]/L$	2.55	2.88	0.50
Volatile solids (percentage)	88.40	88.30	68.40
Biochemical methane potential (mL-CH ₄ /g-dry)	159.80	6.40	12.80

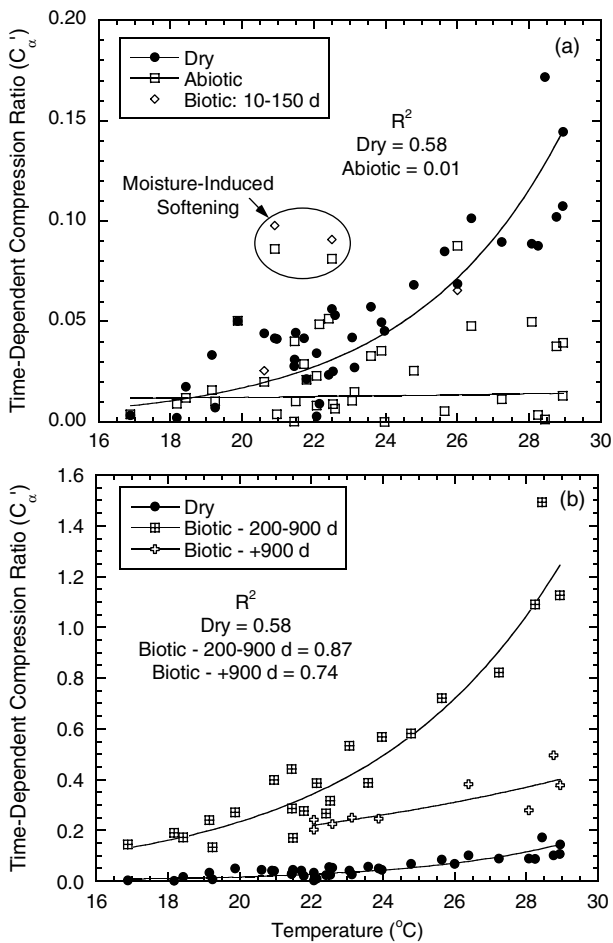


Fig. 9. Monthly time-dependent compression ratios versus monthly average temperature: (a) all three cells; (b) dry and biotic cells; biotic cell data are separated based on time and compression process

Abiotic compression mechanisms include mechanical creep and moisture-induced softening. As shown in Fig. 3(b), the onset of liquid addition and leachate recirculation initiates moisture-induced softening, which increases C'_α above what would be anticipated for waste at a comparable temperature compressing solely due to mechanical creep. Moisture-induced softening increased C'_α in the abiotic and biotic cells approximately two times the C'_α measured in the dry cell at comparable temperatures [Fig. 9(a)].

The predominant compression mechanism in the dry cell was abiotic mechanical creep. Regression parameters for the dry cell [Fig. 9(a)] are both statistically significant (Table 5), which indicates mechanical creep occurs at low temperatures and the rate increases with increased temperature. Thermally activated mechanical creep has been reported by Fox and Edil (1996) for

peat, a close soil analog to MSW. Relationships between compression rate and temperature in Fox and Edil (1996) were also fitted with exponential functions, which support the use of exponential relationships between compression rate and temperature.

The statistical significance of the β parameter for the abiotic regression (Table 5) indicates that mechanical creep occurs in the absence of biological activity. However, the λ parameter for the abiotic regression is not statistically significant (Table 5), indicating temperature did not influence the rate of mechanical creep in the abiotic cell, which is also evident in the low R^2 (0.01) for the abiotic regression. Because the majority of mechanical creep strain accumulated rapidly in the abiotic cell as a result of moisture-induced softening, fluctuations in temperature throughout the experiment did not influence C'_α . This supports the observation that moisture-induced softening accelerates the accumulation of mechanical creep strain, but does not increase the overall magnitude.

Relationships between C'_α and temperature are shown in Fig. 9(b) for the dry and biotic cells. In the presence of biological activity, an increase in temperature results in an increase in C'_α . The rate is more sensitive to temperature when microbial activity is more robust (i.e., C'_α is much less sensitive to temperature for the dry cell due to limited biological activity).

The relationship between C'_α and temperature for the biotic cell shown in Fig. 9(b) is separated into two data sets. The data set for 200–900 days represents compression behavior during the more active period of methane generation (Fig. 5). The data set for +900 days represents compression behavior of decomposed waste when methane yield is essentially exhausted. Regression parameters for both biotic data sets are statistically significant (Table 5).

The data in Fig. 7 indicate that methane flow rate can be an indicator of C'_α during decelerated methane production, when rates of hydrolysis and methanogenesis are comparable. However, the relationship in Fig. 9(b) is applicable for all C'_α and temperature data between 200 and 900 days, regardless of COD removal or methane generation rate. This suggests that for waste undergoing methanogenesis, temperature is a more universal indicator of the rate of biocompression compared with biological indicators of waste decomposition (e.g., gas or leachate characteristics). A similar C'_α -temperature relationship is reported by Bareither et al. (2012) for a field-scale bioreactor experiment. Although the temperature for their field-scale experiment was higher (35–50°C), and the range in C'_α was smaller (0.05–0.4), a positive exponential correlation was determined between C'_α and waste temperature.

Hanson et al. (2010) report that long-term waste temperatures in full-scale landfills are influenced by placement temperatures, which are a function of climatic conditions and operation. Thus, if waste temperatures can be predicted, a C'_α -temperature relationship would be beneficial for estimating C'_α during biocompression. The positive correlation between C'_α and temperature also implies that operational efforts to maintain elevated waste temperatures will accelerate waste settlement, gas generation, and waste decomposition.

Table 5. Regression Parameters and Statistical Significance for Exponential Regressions of Time-Dependent Compression Ratio (C'_α) and Temperature (T) Data Sets; $C'_\alpha = \beta \times e^{(\lambda \times T)}$

Cell	Time period (d)	β	p statistic	λ (1/°C)	p statistic	R^2
Dry	10–1,150	0.0001	1×10^{-12}	0.240	7×10^{-8}	0.58
Abiotic	10–1,150	0.0078	0.002	0.031	0.6	0.01
Biotic	200–900	0.0062	3×10^{-11}	0.180	6×10^{-10}	0.87
	900–1,150	0.0330	0.0002	0.087	0.003	0.74

Note: Regression parameters are statistically significant at the 5% significance level when corresponding p statistics are less than 0.05.

Engineering Implications

Predictions of time-dependent compression strain (ε_{id}) can be obtained with the following equation (Bjarngard and Edgers 1990; El-Fadel and Khoury 2000; Hossain and Gabr 2005):

$$\varepsilon_{id}(t) = C'_{\alpha M} \log \frac{t}{t_M} + C'_{\alpha B} \log \frac{t}{t_B} + C'_{\alpha MF} \log \frac{t}{t_F} \quad (2)$$

where t_M = transition time from immediate compression to mechanical creep, t_B = transition time from mechanical creep to biocompression, t_F = time for completion of biocompression, $C'_{\alpha M}$ and $C'_{\alpha B}$ are defined previously, and $C'_{\alpha MF}$ = compression parameter for final mechanical creep following completion of biocompression. Time in the temporal terms on the right-hand side of Eq. (2) is limited to the period in which each process is active (e.g., $t_B \leq t \leq t_F$ for biocompression).

The applicability of simulating settlement data for the dry and biotic cells using Eq. (2), with C'_α estimated from temperature regressions, was assessed for two scenarios: (1) single C'_α , where a single $C'_{\alpha M}$ and $C'_{\alpha B}$ were computed from average temperatures and (2) monthly C'_α , where monthly C'_α was computed based on monthly average temperatures. The C'_α -temperature regression for the dry data were assumed representative of $C'_{\alpha M}$, and used

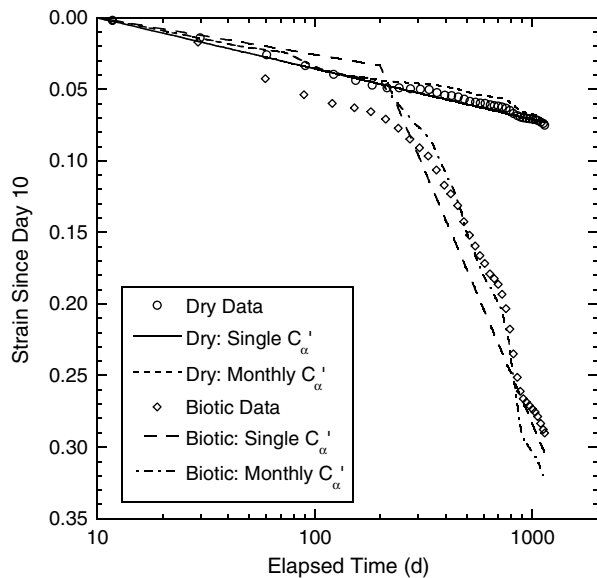


Fig. 10. Predictions of time-dependent settlement in the dry and biotic cells with time-dependent compression ratios (C'_α) computed from C'_α -temperature regressions; mechanical creep ratios ($C'_{\alpha M}$) determined from dry data and biocompression ratios ($C'_{\alpha B}$) from biotic data; single C'_α is the single $C'_{\alpha M}$ and $C'_{\alpha B}$ estimated from average temperature; monthly C'_α is the monthly C'_α estimated from monthly average temperature

for all dry cell data and biotic data between 10 and 200 days. The C'_α -temperature regressions for the biotic data were assumed representative of $C'_{\alpha B}$. A single $C'_{\alpha B}$ was obtained for the first scenario by temporally weighting C'_α , computed from average temperatures between 200 and 900 and 900 and 1,150 days and the corresponding regression equations (Table 5).

Time-dependent strains predicted using Eq. (2) for single and monthly C'_α scenarios are shown in Fig. 10 for the dry and biotic cells. Monthly average strains for these cells are also included in Fig. 10 for comparison. t_M was set equal to 10 days for dry and biotic settlement predictions based on the analysis of immediate compression, and t_B was assumed equal to 200 days for biotic settlement predictions based on observed settlement in Fig. 2. Gourc et al. (2010) linked t_B to the observance of peak methane flow rate; however, this connection was not possible for the biotic cell due to the loss of gas generation data before Day 255.

For the dry cell, compression is predominantly a single mechanism (i.e., abiotic mechanical creep), and both the single and monthly C'_α predictions capture the compression behavior (Fig. 10). However, in the biotic cell, compression occurs due to abiotic and biotic contributions, and thus more deviations exist between the measured and predicted strain compared with the dry cell (Fig. 10). A C'_α representative of moisture-induced softening was not included in the biotic predictions, and the strain increase between 30 and 60 days (Fig. 10) that was caused by liquid addition and leachate recirculation is not captured by the settlement predictions.

A summary of $C'_{\alpha M}$, $C'_{\alpha B}$, R^2 , mean square error, and average bias for the single and monthly C'_α predictions for the dry and biotic cells is in Table 6. The single C'_α prediction for the dry cell yielded a larger R^2 , and an order of magnitude lower sum of squared residuals, mean square error, and average bias compared with the monthly C'_α prediction. Thus, representing the dry data with $C'_{\alpha M} = 0.036$ actually enhanced the statistical significance of the settlement prediction.

The mean square error for the biotic data is reduced by a factor of 1.6 when using monthly C'_α , and the average bias is reduced by a factor of 2.3. However, this enhanced statistical significance required 39 independent C'_α , compared with two C'_α (i.e., $C'_{\alpha M} = 0.026$ and $C'_{\alpha B} = 0.36$) used in the single C'_α prediction. Additionally, the R^2 (Table 6) indicates that both settlement predictions account for greater than 90% of the variance in the biotic data. Using a single $C'_{\alpha M}$ and $C'_{\alpha B}$ to simulate the biotic data is reasonable, considering the marginal increase in statistical significance and the effort associated with identifying 37 additional parameters in the monthly C'_α prediction. This C'_α analysis also indicates that C'_α , due to biocompression ($C'_{\alpha B}$), increases approximately one order of magnitude compared with mechanical creep ($C'_{\alpha M}$) due to biotic waste decomposition.

Table 6. Summary of Mechanical Creep ($C'_{\alpha M}$) and Biocompression ($C'_{\alpha B}$) Ratios, Coefficient of Determination (R^2), Mean Square Error, and Average Bias for the Single and Monthly C'_α Predictions of the Dry and Biotic Time-Dependent Settlement Data

Cell	Prediction	$C'_{\alpha M}$	$C'_{\alpha B}$	R^2	Mean square error	Average bias ^b
Dry	Single C'_α	0.036	–	0.97	6.0×10^{-6}	–0.0015
	Monthly C'_α ^a	0.048 (0.081–0.15)	–	0.89	2.3×10^{-5}	0.0044
Biotic	Single C'_α	0.026	0.36	0.91	6.3×10^{-4}	–0.011
	Monthly C'_α ^a	0.035 (0.014–0.072)	0.42 (0.14–1.2)	0.95	4.0×10^{-4}	–0.0047

^aAverage C'_α and range in parentheses.

^bBias is measured – predicted.

Summary and Conclusions

Abiotic and biotic compression of MSW was assessed in three large-scale laboratory experiments. These experiments were operated under the following conditions: (1) no liquid addition (dry), (2) liquid addition spiked with biocide (abiotic), and (3) leachate recirculation (biotic). Experiments were conducted for 1,150 days; settlement, gas composition and production, and leachate chemistry were monitored. The following conclusions are drawn from this study:

- The biocide used in the abiotic cell effectively inhibited biological activity.
- Decomposition of C and H was the predominant pathway for methane generation in the biotic cell; approximately 95% of the difference between BMPs for waste recovered from the dry and biotic cells was accounted for in C and H loss.
- Time-dependent compression strain at the end of the test period in the biotic cell was > 3.5 times the strain in the dry and abiotic cells due to biotic waste decomposition.
- Moisture-induced softening in the abiotic and biotic cells doubled the time-dependent compression ratio (C'_α), representative of mechanical creep in the dry cell. This softening process is finite (lasting only 3 months), accelerates the accumulation of mechanical creep, but does not increase the total strain due to mechanical creep.
- Methane flow rate was unrelated to temperature when substrates for methanogenesis were abundant in the leachate, i.e., during high rates of COD removal. However, the methane flow rate was dependent on temperature when COD removal was low and methanogenesis was dependent on the rate of solids hydrolysis.
- During low COD removal, C'_α was related to the methane flow rate, indicating that elevated waste temperatures during anaerobic MSW decomposition enhanced solids decomposition, methane generation, and waste settlement, and yield a larger C'_α .
- C'_α , due to mechanical creep in the absence of liquid addition, and C'_α , due to biocompression, increased exponentially with temperature. Temperature was found to be a more universal indicator of C'_α during biocompression compared with biological indicators of waste decomposition (e.g., gas or leachate characteristics).
- C'_α , due to biocompression, is approximately an order of magnitude larger than C'_α due to mechanical creep.

Acknowledgments

Financial support was provided by the University of Wisconsin-North Carolina State University bioreactor partnership (www.bioreactorpartnership.org), which was sponsored by the U.S. National Science Foundation (Grant No. EEC-0538500) and a consortium of industry partners (CH2MHill, Geosyntec Consultants, Republic Services, Veolia Environmental Services, Waste Connections Inc., and Waste Management) through the National Science Foundation's Partnerships for Innovation Program. Additional thanks are extended to Ronald Breitmeyer (Exponent Inc., USA) and Suna Ertes (Sakarya University, Turkey) for assistance with laboratory testing.

References

Bareither, C. A., Benson, C. H., Barlaz, M. A., Edil, T. B., and Tolaymat, T. M. (2010). "Performance of North American bioreactor landfills: I. leachate hydrology and waste settlement." *J. Environ. Eng.*, 136(8), 824–838.

Bareither, C. A., Breitmeyer, R. J., Benson, C. H., Barlaz, M. A., and Edil, T. B. (2012). "Deer Track Bioreactor Experiment: A field-scale evaluation of municipal solid waste bioreactor performance." *J. Geotech. Geoenviron. Eng.*, 138(6), 658–670.

Barlaz, M. A. (1997). "Microbial studies of landfills and anaerobic refuse decomposition." *Manual for environmental microbiology*, American Society of Microbiology, Washington, D.C., 541–557.

Barlaz, M. A. (2006). "Forest products decomposition in municipal solid waste landfills." *Waste Manage.*, 26(4), 321–333.

Barlaz, M. A., Ham, R. K., and Schaefer, D. M. (1990). "Methane production from municipal refuse: A review of enhancement techniques and microbial dynamics." *Manual for environmental microbiology*, American Society of Microbiology, Washington, D.C., 541–557.

Barlaz, M. A., Schaefer, D. M., and Ham, R. K. (1989). "Bacterial population development and chemical characteristics of refuse decomposition in a simulated sanitary landfill." *Appl. Environ. Microbiol.*, 55(1), 55–65.

Bilgili, M. S., Demir, A., and Özkaya, B. (2007). "Influence of leachate recirculation on aerobic and anaerobic decomposition of solid wastes." *J. Hazard. Mater.*, 143(1–2), 177–183.

Bjarngard, A., and Edgers, L. (1990). "Settlement of municipal solid waste landfills." *Proc., 13th Annual Madison Waste Conf.*, Dept. of Engineering, Professional Development, Univ. of Wisconsin, Madison, Madison, WI, 192–205.

Cecchi, F., Mata-Alvarez, J., Pavan, P., Vallini, G., and De Poli, F. (1992). "Seasonal effects on anaerobic digestion of the source sorted organic fraction of municipal solid waste." *Waste Manage. Res.*, 10(5), 435–443.

Chugh, S., Clarke, W., Pullammanappallil, P., and Rudolph, V. (1998). "Effect of recirculated leachate volume on MSW degradation." *Waste Manage. Res.*, 16(6), 564–573.

Clescerl, L. S., Greenberg, A. E. and Eaton, A. D., eds. (1999). *Standard methods for the examination of water and wastewater*, 20th Ed., American Public Health Association, Washington, DC.

Colberg, P. J. (1988). "Anaerobic microbial degradation of cellulose, lignin, oligolignols, and monoaromatic lignin derivatives." *Biology of anaerobic microorganisms*, A. J. B. Zehnder, ed., Wiley-Liss, New York, 333–372.

Davis, M. W. (1998). "A rapid modified method for compositional carbohydrate analysis of lignocellulosics by high pH anion-exchange chromatography with pulsed amperometric detection (HPAEC/PAD)." *J. Wood Chem. Technol.*, 18(2), 235–252.

Edil, T., Ranguette, V., and Wuellner, W. (1990). "Settlement of municipal refuse." *Geotechnics of Waste Fills-Theory and Practice, STP 1070*, A. O. Landva and G. D. Knowles, eds., ASTM, West Conshohocken, PA, 225–239.

El-Fadel, M., and Houry, R. (2000). "Modeling settlement in MSW landfills: A critical review." *Crit. Rev. Environ. Sci. Technol.*, 30(3), 327–361.

Farquhar, G. J., and Rovers, F. A. (1973). "Gas production during refuse decomposition." *Water Air Soil Pollut.*, 2(4), 483–495.

Fox, P. J., and Edil, T. B. (1996). "Effects of stress and temperature on secondary compression of peat." *Can. Geotech. J.*, 33(3), 405–415.

Gourc, J. P., Staub, M. J., and Conte, M. (2010). "Decoupling MSW settlement into mechanical and biochemical processes—modeling and validation on large-scale setups." *Waste Manage.*, 30(8–9), 1556–1568.

Ham, R. K., and Bookter, T. J. (1982). "Decomposition of solid waste in test lysimeters." *J. Environ. Eng. Div.*, 108(6), 1147–1170.

Hanson, J. L., Yesiller, N., and Oettle, N. K. (2010). "Spatial and temporal temperature distributions in municipal solid waste landfills." *J. Environ. Eng.*, 136(8), 804–814.

Hao, Y. J., Wu, W. X., Wu, S. W., Sun, H., and Chen, Y. X. (2008). "Municipal solid waste decomposition under oversaturated condition in comparison with leachate recirculation." *Process Biochem.*, 43(1), 108–112.

Hartz, K. E., Klink, R. E., and Ham, R. K. (1982). "Temperature effects: Methane generation from landfill samples." *J. Environ. Eng. Div.*, 108(4), 629–638.

- Hossain, M. S., and Gabr, M. A. (2005). "Prediction of municipal solid waste landfill settlement with leachate recirculation." *Proc. Geo-Frontiers, GSP No. 142, Waste Containment and Remediation*, ASCE, Austin, TX, 1–14.
- Hossain, M. S., Gabr, M. A., and Barlaz, M. A. (2003). "Relationship of compressibility parameters to municipal solid waste decomposition." *J. Geotech. Geoenviron. Eng.*, 129(12), 1151–1158.
- Hull, R. M., Krogmann, U., and Strom, P. F. (2005). "Composition and characteristics of excavation materials from a New Jersey landfill." *J. Environ. Eng.*, 131(3), 478–490.
- Ivanova, L. K., Richards, D. J., and Smallman, D. J. (2008). "The long-term settlement of landfill waste." *Water Resour. Manage.*, 161(3), 121–133.
- Kang, S. T., Hang, S. S., Lee, C. Y., and Lee, N. H. (1997). "Relationship between biological decomposition and landfill settlement at various leachate recirculation rates." *Proc., 7th KAIST-NTU-KU Tri-Lateral Seminar/Workshop on Environ. Eng.*, Kyoto, Japan, 29–31.
- Kettunen, R. H., and Rintala, J. A. (1997). "The effect of low temperature (5–29°C) and adaptation on the methanogenic activity of biomass." *Appl. Microbiol. Biotechnol.*, 48(4), 570–576.
- Kim, J., and Pohland, F. G. (2003). "Process enhancement in anaerobic bioreactor landfills." *Water Sci. Technol.*, 48(4), 29–36.
- Levén, L., Eriksson, A. R. B., and Schnürer, A. (2007). "Effect of process temperature on bacterial and archaeal communities in two methanogenic bioreactors treating organic household waste." *FEMS Microbiol. Ecol.*, 59(3), 683–693.
- Marques, A. C. M., Filz, G. M., and Vilar, O. M. (2003). "Composite compressibility model for municipal solid waste." *J. Geotech. Geoenviron. Eng.*, 129(4), 372–378.
- Noike, T., Endo, G., Chang, J., Yaguchi, J., and Matsumoto, J. (1985). "Characteristics of carbohydrate degradation and the rate-limiting step in anaerobic digestion." *Biotechnol. Bioeng.*, 27(10), 1482–1489.
- Olivier, F., and Gourc, J. P. (2007). "Hydro-mechanical behavior of municipal solid waste subject to leachate recirculation in a large-scale compression reactor cell." *Waste Manage.*, 27(1), 44–58.
- Park, H. I., and Lee, S. R. (1997). "Long-term settlement behavior of landfills with refuse decomposition." *J. Solid Waste Technol. Manage.*, 24(4), 159–165.
- Pavlostathis, S. G., and Giraldo-Gomez, E. (1991). "Kinetics of anaerobic treatment." *Water Sci. Technol.*, 24(8), 35–59.
- Pettersen, R. C., and Schwandt, V. (1991). "Wood sugar analysis by anion chromatography." *J. Wood Chem. Technol.*, 11(4), 495–501.
- Pohland, F. G. (1980). "Leachate recycle as landfill management option." *J. Environ. Eng. Div.*, 106(6), 1057–1069.
- Pohland, F. G., and Kim, J. C. (1999). "In situ anaerobic treatment of leachate in landfill bioreactors." *Water Sci. Technol.*, 40(8), 203–210.
- Rao, M. S., and Singh, S. P. (2004). "Bioenergy conversion studies of organic fraction of MSW: Kinetic studies and gas yield-organic loading relationships for process optimization." *Bioresour. Technol.*, 95(2), 173–185.
- Sharma, H. D., and De, A. (2007). "Municipal solid waste landfill settlement: Postclosure perspectives." *J. Geotech. Geoenviron. Eng.*, 133(6), 619–629.
- Sivakumar Babu, G. L. S., Reddy, K. R., Chouskey, S. K., and Kulkarni, H. S. (2010). "Prediction of long-term municipal solid waste landfill settlement using constitutive model." *Pract. Period. Hazard. Toxic Radioact. Waste Manage.*, 14(2), 139–150.
- Sowers, G. (1973). "Settlement of waste disposal fills." *Proc., 8th Int. Conf. on Soil Mech. and Foundation Eng.*, Balkema, Rotterdam, 22, 207–210.
- Vavilin, V. A., Rytov, S. V., and Lokshina, L. Ya. (1996). "A description of hydrolysis kinetics in anaerobic degradation of particulate organic matter." *Bioresour. Technol.*, 56(2–3), 229–237.
- Wall, D., and Zeiss, C. (1995). "Municipal landfill biodegradation and settlement." *J. Environ. Eng.*, 121(3), 214–224.
- Wang, Y. S., Byrd, C. S., and Barlaz, M. A. (1994). "Anaerobic biodegradability of cellulose and hemicellulose in excavated refuse samples." *J. Ind. Microbiol.*, 13(3), 147–153.
- Westlake, K., Archer, D. B., and Boone, D. R. (1995). "Diversity of cellulolytic bacteria in landfill." *J. Appl. Bacteriol.*, 79(1), 73–78.
- Zehnder, A. J. B. (1978). "Ecology of methane formation." *Water pollution microbiology*, R. Mitchell, ed., Vol. 2, Wiley, New York, 349–376.

Copyright of Journal of Geotechnical & Geoenvironmental Engineering is the property of American Society of Civil Engineers and its content may not be copied or emailed to multiple sites or posted to a listserv without the copyright holder's express written permission. However, users may print, download, or email articles for individual use.